

Electrorheological Properties of Kaolinite, Polyindole, and Polyindole/Kaolinite Composite Suspensions

Yasin Arslan,¹ Halil Ibrahim Unal,² Hasim Yilmaz,³ Bekir Sari²

¹Chemistry Department, METV, Ankara 06500, Turkey

²Chemistry Department, Science Faculty, Gazi University, Teknikokullar, Ankara 06500, Turkey

³Chemistry Department, Science Faculty, Harran University, Osmanbey, Sanliurfa 63190, Turkey

Received 28 June 2006; accepted 18 January 2007

DOI 10.1002/app.26197

Published online 8 March 2007 in Wiley InterScience (www.interscience.wiley.com).

ABSTRACT: In this study, polyindole (PIN) and polyindole/kaolinite (PIN/KAO) composite were synthesized by free radical polymerization using FeCl₃ as an initiator. Average particle sizes (d_{50}) of PIN and PIN/KAO composite were determined by dynamic light scattering (DLS) as 7.2 and 6.2 μm , respectively. The samples were characterized by FTIR, elemental analysis, DSC/TGA and SEM measurements. Suspensions of KAO, PIN, and PIN/KAO composite were prepared in silicone oil (SO) and the sedimentation stabilities were determined. Electrorheological

(ER) properties of these suspensions were studied as a function of dispersed phase concentration, shear rate, shear stress, and temperature; and yield stresses and excess shear stresses determined. Further, dielectric properties of KAO, PIN, and PIN/KAO composite were investigated. © 2007 Wiley Periodicals, Inc. *J Appl Polym Sci* 104: 3484–3493, 2007

Key words: kaolinite; polyindole; polyindole/kaolinite composites; electrorheological suspensions

INTRODUCTION

Electrorheological (ER) fluids composed of a suspension of micron-sized particles in a nonconducting fluid to form fibrillated particle structures, which are caused by the dielectric constant mismatch of the particles and the insulating oil, in strong electric fields.^{1,2} Thus, it is quite natural that dielectric polarization theory appeared, because ER behavior was closely related to dielectric phenomena, and among various polarizations, interfacial polarization is assumed to be responsible for ER phenomena.³ To overcome the shortcomings (thermal instability and corrosion) that wet-base ER systems possess, various dry-base ER systems have been investigated with anhydrous particles, including zeolite,⁴ carbonaceous particle, and intrinsically polarizable semiconducting polymers.⁵ Special attention has been paid to the polymer-based ER materials. Examples include: acene quinone radical polymers,⁶ polyaniline,^{7,8} copolyaniline,⁹ polyphenylenediamine,¹⁰ poly(2-acrylamido-2-methyl-1-propane sulfonic acid),¹¹ polystyrene-*block*-polyisoprene,¹² polyaniline nanocomposite,¹³ polyacrylonitrile/diatomite composites,¹⁴ poly

(Li-HEMA)-*co*-poly(4-vinyl pyridine) copolymeric ionomer,^{15,16} PMMA-*b*-PSt,¹⁷ poly(Li-2-hydroxyethyl methacrylate)/SO systems.¹⁸ The difference between dry-base and wet-base systems is the carrier species for particle polarization. The particle chain structure is formed by the migration of ions in the absorbed water in wet-base ER fluids, whereas the electrons move inside the molecules of the particles in the dry-base ER fluids.

There is also a need for fluids with enhanced colloidal stability against sedimentation and sludge deposits formation.¹⁹ Most of the studies on the literature are focused on the ER activity of acrylate salts and zeolitic materials, and very few of these researchers have investigated the influence of colloidal stability of suspensions. Another target is, for ER fluids, with long service stabilities, particularly at high temperatures and rigid environmental conditions.²⁰

ER active materials possess either branched polar groups such as amine ($-\text{NH}_2$), hydroxyl ($-\text{OH}$) and amino-cyano ($-\text{NHCN}$), or semiconducting repeated groups. The polar groups may affect the ER behavior by playing a role of the electronic donor under imposed electric field. The chemical structure of the organic materials is, therefore, an important factor in the ER performance.

There are very wide ranges of potential applications for ER fluids in areas such as: vibration dampers, robotics, hydraulics, shock absorbers, ER valves, couplings, and automotive industries.²¹ The patent

Correspondence to: H. I. Unal (hiunal@gazi.edu.tr).

Contract grant sponsor: State Planning Organization; contract grant number: DPT, 2001 K 120580.

Contract grant sponsor: Gazi University.

literature on the subject suggests a growing interest in such devices after a period of research and assessment.^{22,23} A major limiting factor is still the need for fluids with better overall performance. Important factors influencing the ER effect are electric field strength, field frequency; shear rate, fluid composition, temperature, colloidal stability, and presence of a polar promoter.²⁴

Clay minerals have recently been introduced into the field of composites because of their small particle size and intercalation properties, especially in the application of reinforcement of materials with polymers.²⁵

In this research, polyindole (PIN) and polyindole/kaolinite (PIN/KAO) composite were chemically synthesized; their characterization, dielectric, and ER properties were investigated. To prepare a potential industrial ER fluid we have also tested the suspensions for colloidal and thermal stability.

EXPERIMENTAL

Materials

Indole, (Merck), iron (III) chloride (FeCl_3 , Aldrich), silicon oil (Aldrich), and acetonitrile (Merck) were used as received.

The physical properties of silicone oil are given below:

Viscosity: 200 mPa s (at 25°C), density: 0.965 g/cm³ (at 25°C), dielectric constant: 2.6, boiling point: 140°C, vapor pressure 5 mmHg (at 20°C).

The physical properties of KAO (kindly provided by Omya Mining Co. of Istanbul) are given below:

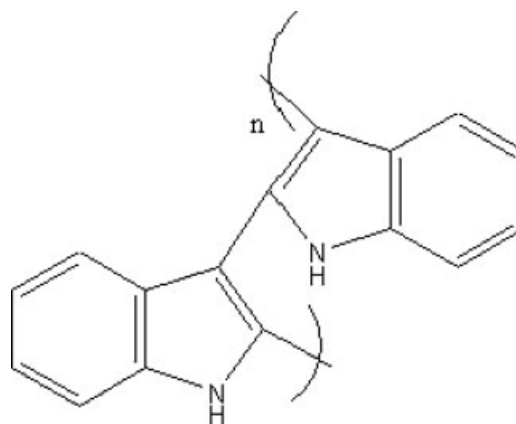
Chemical formula: $\text{Al}_2\text{Si}_2\text{O}_5(\text{OH})_4$; class: silicate; color: white, density: 2.6 g cm⁻³, refractive index: 1.55, hardness (Mohs): 2.5, average diameter (d_{50}): 4.8 μm .

Chemical composition: Al_2O_3 : >15%, SiO_2 : <76%, Fe_2O_3 : <0.5%.

KAO was chosen as a clay material to prepare a composite with PIN, because it is a ubiquitous mineral in sediment systems, cheap and easy to obtain.²⁶

Synthesis of PIN

PIN was synthesized by radicalic mechanism at 55°C, using FeCl_3 as an initiator. Firstly, 0.092 mol FeCl_3 was dissolved in 100 mL acetonitrile (CH_3CN) in a three necked flask, and then 0.03 mol indole monomer (also dissolved in 25 mL CH_3CN) was added drop-wise into this solution under N_2 gas atmosphere, and the polymerization reaction started (Scheme 1). The polymerizing solution was kept stirring for 24 h. Then, the crude PIN was subjected to vacuum filtration, washed several times with hot water, to remove any impurities present, and dried



Scheme 1 The structure of PIN.

at 70°C for 48 h under 15 mmHg in a vacuum oven. The product was recovered with 79% yield.

Synthesis of PIN/KAO composite

PIN/KAO composite was synthesized by a free radicalic mechanism at 55°C, using FeCl_3 as an initiator. Firstly, 0.092 mol FeCl_3 was dissolved in 100 mL CH_3CN in a three necked flask, and then 1.5 g KAO was added into this solution and finally 0.03 mol indole monomer (dissolved in 25 mL CH_3CN) was added drop-wise into this solution under N_2 gas atmosphere, and the composite formation reaction started. The reaction was kept stirring for 24 h. Then PIN/KAO composite was subjected to vacuum filtration, washed several times with hot water, to remove any impurities present, and vacuum dried at 70°C for 48 h under 15 mmHg. The product was recovered with 69% yield. The composition of the PIN/KAO composite was determined gravimetrically as 62% PIN and 38% KAO.

Characterization

Particle size measurements

Particle sizes of PIN, and PIN/KAO composite were determined using a Malvern Mastersizer E, version 1.2b particle size analyzer according to Fraunhofer scattering. During the measurements, some samples were dispersed in ethanol and stirred at a constant temperature of $(20 \pm 0.1)^\circ\text{C}$. The data collected were evaluated according to Fraunhofer diffraction theory by the Malvern software computer.²⁷

FTIR spectroscopy and elemental analysis

KAO, PIN, and PIN/KAO composite were characterized before ER measurements to be carried out by elemental analysis and FTIR spectroscopy.

The FTIR spectra of PIN, KAO and PIN/KAO were recorded using a Mattson Model 1000 spectrometer (U.K). Samples were analyzed as KBr (spectrophotometric grade) discs.

Elemental analysis was performed by TUBITAK's microanalytical laboratory using a LECO-CHNS-9320 model elemental analyzer (USA), and the results were used to check purity of the samples by comparison with the calculated compositions.

DSC/TGA measurements

Perkin-Elmer-Pyris Diamond TG-DSC Model instrument (USA) was used for thermal analysis of composite. The samples were heated up to 900°C with a heating rate of 10°C/min under nitrogen atmosphere.

SEM measurements

The micro-structure of PIN/KAO composite was recorded on a JEOL JSM 6360 LV (JAPAN) scanning electron microscope (SEM).

Conductivity measurements

The current-potential measurements were performed on PIN and PIN/KAO composite discs (20 mm × 5 mm × 1 mm), with a Keithley 220 programmable current source and a Keithley 199 digital multimeter (USA) at an ambient temperature. The capacitance, C , of ER particles was measured with an HP 4192 A LF Impedance Analyzer (USA) at a frequency of 1.0 MHz at constant temperature (20 ± 0.1)°C.

Preparation of suspensions

Suspensions of PIN, KAO, and PIN/KAO composite were prepared in silicon oil (SO) at a series of particle concentrations ($c = 5\text{--}30$ m/m, %), by dispersing definite amount of solid particles in calculated amount of SO according to the formula:

$$(m/m, \%) = \left[\frac{m_{\text{solid particles}}}{(m_{\text{solid particles}} + m_{\text{oil}})} \right] \times 100 \quad (1)$$

Sedimentation stability measurements of suspensions

Sedimentation stabilities of PIN/SO and PIN/KAO/SO composite suspensions were determined at (25 ± 0.1)°C. Glass tubes containing the suspensions, prepared at a series of solid particle concentrations ($c = 5\text{--}30$ m/m, %), were immersed into a constant temperature water bath and formation of first pre-

cipitates was recorded to be the indication of colloidal instability.

ER measurements

Flow rate measurements

The experimental determination of flow behavior and viscoelastic material properties, which influence processing technology and polymer stability and consistency, were aimed. Flow rate measurements of PIN/SO, KAO/SO, and PIN/KAO/SO composite suspensions were carried out between two brass electrodes. The gap between the electrodes was 0.5 cm, the width of the electrodes was 1.0 cm, and the height of ER liquid on the electrodes was 5.0 cm. During the measurements these electrodes were connected to an external high voltage dc electric source (0–12.5 kV, with 0.5 kV increments, Fug electronics HCL-14, Germany) and a digital voltmeter. The electrodes were dipped into a vessel containing the suspension and after a few seconds the vessel was removed and the flow time for complete drainage measured, using a digital stop-watch under $E = 0$ kV/mm and E (0 kV/mm conditions, respectively). This procedure was repeated for each suspension concentration under various electric field strengths.

Electro-rheometer measurements

PIN, KAO and PIN/KAO composite were dispersed in SO and stirred fully (solid particle fractions of 5–30%) to prepare all the ER suspension samples. The ER experiments were performed using a Thermo-Haake RS600 torque rheometer, equipped with an ER adapter. The apparatus can work under a given temperature and plate clearance to measure the shear stress and apparent viscosity of a fluid at various shear rates, and it has the function of controlled rate (CR), controlled stress (CS) and oscillation operating modes.

In this study, measurements were carried out using a PP35 ER sensor system, which is a pair of parallel plates and the gap between the plates was 1.000 mm. For each measurement, a suspension sample was placed between the lower and upper plates at constant temperature and the upper plate was rotated at a predetermined shear rate, while the down plate kept stationary. The applied shear rate ranges were 0–1000 s⁻¹. During the ER measurements, shear stresses and viscosities of the samples were determined under various external applied dc electric field strengths ($E = 0.0\text{--}2.0$ kV/mm, with 0.5 kV/mm increments) at various temperatures ($T = 25\text{--}125^\circ\text{C}$, with 25°C increments). The voltage used in these experiments was supplied by a 0–12.5 kV dc electric field generator (Fug electronics

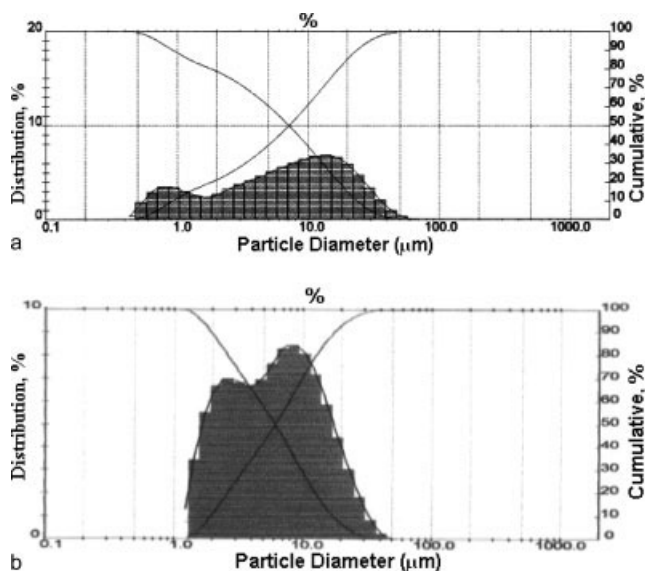


Figure 1 Particle size distribution of (a) PIN and (b) PIN/KAO composite.

HCL-14, Germany), which enabled resistivity to be created during the experiments.

RESULTS AND DISCUSSION

Characterization

The characterization studies of KAO, PIN, and PIN/KAO composite is discussed below:

Average particle sizes (d_{50}) of PIN [Fig. 1(a)] and PIN/KAO composites [Fig. 1(b)] were determined from particle size measurements, according to Fraunhofer diffraction theory.²⁷ As reflected from the particle size distribution histograms, PIN was accumulated around 7.2 μm and that of PIN/KAO

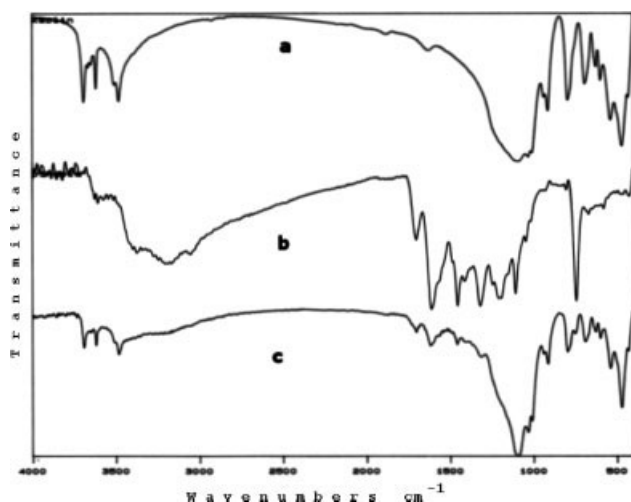


Figure 2 FTIR spectrum of (a) KAO, (b) PIN, (c) PIN/KAO composite.

TABLE I
The Elemental Analysis Results of PIN

Element	C (%)	H (%)	N (%)
Experimental	82.30	6.15	11.55
Calculated	82.05	5.98	11.97

composite was accumulated around 6.2 μm . The average particle size of KAO was provided to be $d_{50} = 4.8 \mu\text{m}$, by the Omya Mining Co.

FTIR spectra of KAO, PIN, and PIN/KAO composite (Fig. 2) showed the expected distinctive absorptions. The FTIR absorptions of KAO [Fig. 2(a)] at 3500, 3520, 3620, and 3698 cm^{-1} were assigned to the inner hydroxyl group stretching.

The FTIR absorptions obtained for PIN [Fig. 2(b)] in this study were similar to those reported in the literature for homopolyindole.^{28,29}

The FTIR spectrum of PIN/KAO composite [Fig. 2(c)] at 3698 cm^{-1} , 1612 cm^{-1} , and 3050–3100 cm^{-1} are typical of $-\text{OH}$, $-\text{C}=\text{C}-$, and $-\text{C}-\text{H}$ stretching vibrations. The band at 3320 cm^{-1} is assigned to the $\text{N}-\text{H}$ stretching. The FTIR spectra of composite supported that the composite synthesis was successful.

The experimental and calculated compositions obtained from elemental analysis of the PIN and PIN/KAO composite are given in Table I. The measured compositions agree very well with the calculated values. These results also support that PIN and PIN/KAO composite are successfully synthesized.

Thermal analysis results of PIN and PIN/KAO composites are given in Table II and corresponding curves are depicted in Figure 3(a,b). As seen from Figure 3(a), PIN decomposes with three step weight losses. The first step weight loss occurs between 100 and 180 $^{\circ}\text{C}$, which corresponds to the adsorbed volatile molecules, and low molecular weight segments in polymer matrix. The second weight loss step occurs between 230 and 315 $^{\circ}\text{C}$, which can be attributed to the loss of the dopant salts bonded to the polymer chain. The third decomposition step occurs between 315 and 535 $^{\circ}\text{C}$, which corresponds to the

TABLE II
Thermal Analysis Results of PIN and PIN/KAO Composite

Sample	T_i ($^{\circ}\text{C}$)	T_{max} ($^{\circ}\text{C}$)	T_f ($^{\circ}\text{C}$)	$T_{d(1/2)}$ ($^{\circ}\text{C}$)	Residue at 800 $^{\circ}\text{C}$ (m/m %)
PIN	100	130	180	440	50
	230	246	315		
	315	490	535		
PIN/KAO	678	722	745	720	53

T_i , Initial decomposition temperature; T_{max} , Maximum decomposition temperature; T_f , Final decomposition temperature; $T_{d(1/2)}$, Half decomposition temperature.

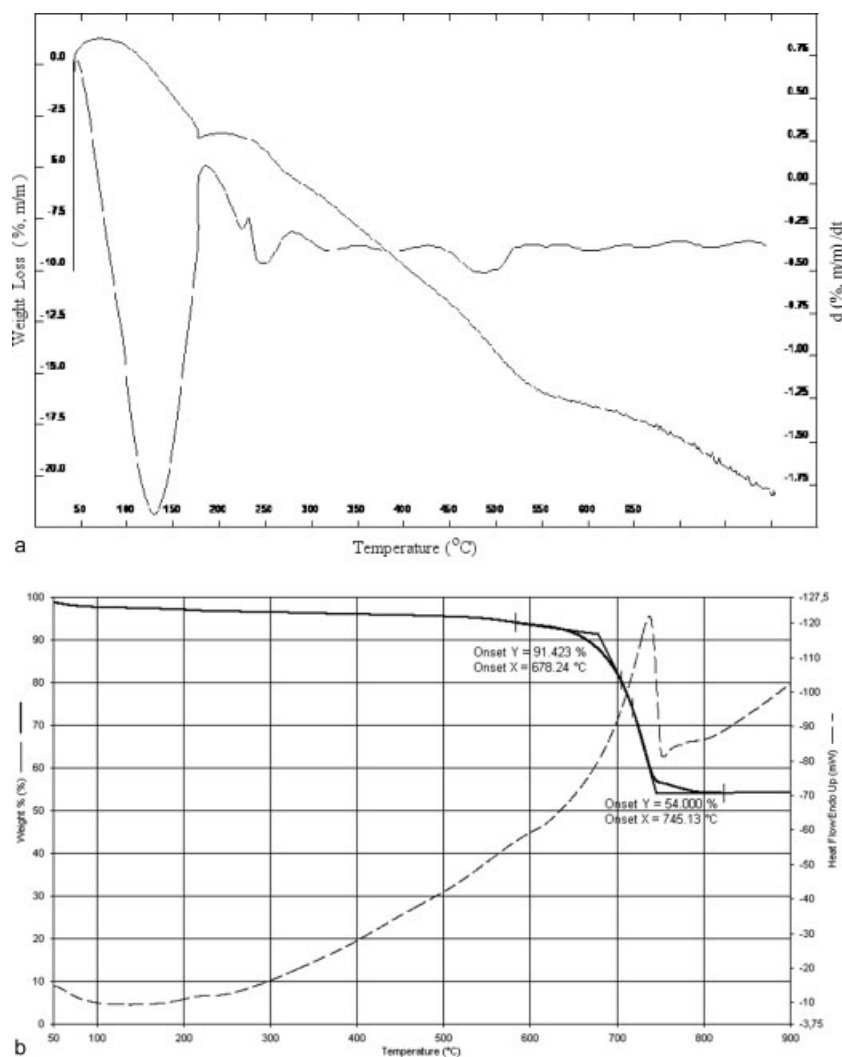


Figure 3 (a) TGA of PIN, (b) DSC/TGA curves of PIN/KAO composite.

decomposition of polymer skeleton after the removal of dopant salts from the polymer structure.³⁰

TGA result of PIN/KAO [Fig. 3(b)] exhibits a one step weight loss. According to TGA curve it was found that it has a thermal stability up to 670°C. The initial decomposition temperature (T_i) of PIN/KAO composite was determined to be 678°C. The maximum decomposition temperature (T_{max}) and the final decomposition temperature (T_f) of PIN/KAO composite were found to be 715°C and 745°C, respectively. DSC curve did not show any thermal transition temperature, but it was demonstrated a sharp endothermic phase change at 745°C. From thermal analysis results, it was concluded that PIN/KAO composite has high thermal stability.

The SEM of PIN/KAO composite demonstrates both of granular-porous and sponge-like structures (Fig. 4). From the SEM micrograph and thermal analysis results it can be concluded that PIN/KAO composite is a compatible mixture.

Conductivity and dielectric measurements

The conductivities of PIN, KAO and PIN/KAO composite were determined to be $2.0 \times 10^{-7} \text{ S cm}^{-1}$, $8.3 \times 10^{-4} \text{ S cm}^{-1}$ and $4.6 \times 10^{-7} \text{ S cm}^{-1}$, in turn. That is well in the range of the expected conductivity ($1 \times 10^{-3} \text{ to } 1 \times 10^{-8} \text{ S m}^{-1}$) of ER particles, reported in the literature.³¹

The composite has not only electronic conductivity, due to PIN units, but also ionic participation of the KAO part. As expected, the driving force behind the ER activity of these systems is the polarization of ions suspended inside the suspensions.³²

The dielectric constants were derived from the measured capacitance (C) according to the conventional relation,

$$\varepsilon = Cd/\varepsilon_0S \quad (2)$$

where ε_0 is the dielectric constant of the vacuum, (i.e., $8.85 \times 10^{-12} \text{ F m}^{-1}$), d is the distance of the

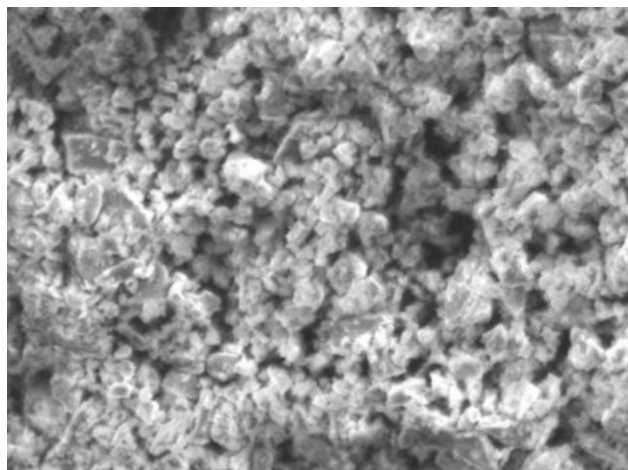


Figure 4 SEM micrograph of PIN/KAO composite (800 \times).

gap between the electrodes, and S is the contact area of the electrodes. The permittivities of PIN and PIN/KAO composite were found to be 5.39 and 5.63, respectively. As suggested by Hao³¹ the permittivity of an ER suspension should lie between $2.0\text{--}1.0 \times 10^4$.

Sedimentation stability of suspensions

Despite the recent activities surrounding ER fluids and ER effect, little efforts have focused on the colloidal stability of these suspensions. Few investigations probe the colloid chemistry of ER fluids.^{15,33} When the density of particles is not as same as that of medium, the particles with micron order size will settle down according to the Stoke's law.³⁴ To solve the traditional problem of particle sedimentation, several researchers have developed different solutions.³⁵ Density mismatch between dispersed and continuous phase in the suspension plays an important role in sedimentation stability of an ER fluid. We have determined the densities of PIN, KAO and PIN/KAO composite as 0.98, 2.6, and 1.25 g cm⁻³, respectively. The density of SO was 0.965 g cm⁻³ (at 25°C).

Sedimentation stabilities of PIN and PIN/KAO suspensions were determined in SO at 25°C and the results obtained are tabulated in Table III. The sedimentation stability of suspensions increased with decreasing particle concentration. Although the den-

sity of PIN was smaller than the density of PIN/KAO composite, the maximum sedimentation stability was observed to be 72 days at $c = 5\%$ particle concentration for PIN/KAO composite/SO suspension. This may be attributed to the smaller particle size distribution of PIN/KAO composite ($d_{50} = 6.2 \mu\text{m}$), than PIN ($d_{50} = 7.2 \mu\text{m}$). The observed 72 days of colloidal stability is a sufficient result from an industrial point of view. The lowest sedimentation stability was observed to be 21 days at 30% particle concentration for PIN(SO suspension).

Electrorheology

Since the ER phenomena is widely attributed to the chaining of micron-sized polarisable particles, when subjected to an external electric field, flow rate and ER studies are conducted to observe the viscosity change at flow and ER response of KAO(SO, PIN(SO and PIN/KAO(SO composite suspensions.

Flow rate measurements

To observe the effect of dc electric field on ER activity; flow rate measurements are carried out on the KAO(SO, PIN(SO and PIN/KAO(SO composite suspensions. For this purpose, the flow times of these suspensions were measured at ambient temperature and constant particle concentration ($c = 15\%$, m/m) under $E = 0$ kV and $E = 0$ kV conditions. Flow times of suspensions were first shown little increase with rising electric field strength up to threshold energies ($E_t = 1.5$ kV/mm), and then sharp increases were observed for all the three suspensions (Fig. 5). Maximum flow times (t_{flow}) of the suspensions reached at $E = 2.0$ kV/mm were changed as follows: KAO/SO (346 s) < PIN/SO (420 s) < PIN/KAO/SO system (598 s).

Flow times given for the suspensions are the maximum flow times, which could be observed under the external applied electric field. When electric field was further increased, a highly stronger bridge formation was occurred for all the suspensions and no flow was observed. Similar behaviors were reported for sepiolite ($t_{\text{flow}} = 168$ s),³⁶ diatomite and diatomite/polyacrylonitrile composite ($t_{\text{flow}} = 150$ s)¹⁵ suspensions both prepared in SO.

TABLE III
Sedimentation Stability Results of PIN and PIN/KAO Composite Suspensions

Concentration (m/m)	%30	%25	%20	%15	%10	%5
PIN	21 days	30 days	46 days	55 days	58 days	63 days
PIN/KAO Composite	26 days	38 days	52 days	61 days	69 days	72 days

($T = 20^\circ\text{C}$).

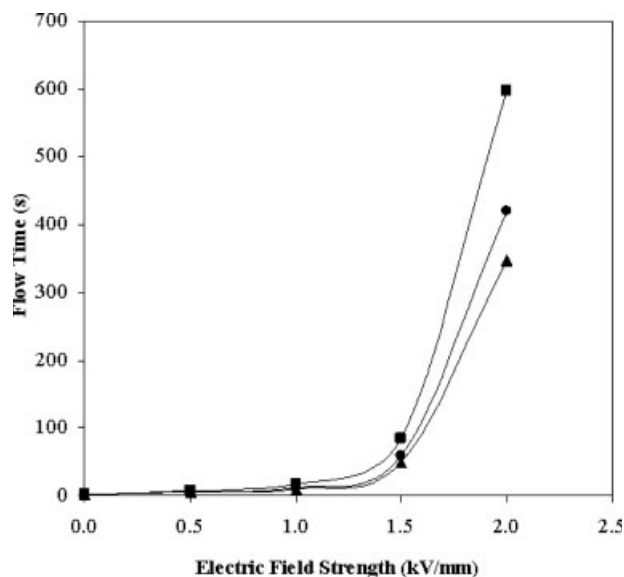


Figure 5 Effect of electric field strength on flow time. (■) PIN/KAO, (●) PIN, (▲) KAO.

Effect of concentration on electric field viscosity

The change in electric field viscosity with suspension concentration of KAO, PIN, and PIN/KAO composite particles dispersed in SO at various particle sizes, constant shear rate ($\dot{\gamma} = 1.0 \text{ s}^{-1}$), electric field strength ($E = 2.0 \text{ kV/mm}$) and temperature ($T = 25^\circ\text{C}$) is depicted in Figure 6. When increasing the KAO, PIN, and PIN/KAO composite particle concentration, the flow curves of suspensions in the presence of electric field become more pseudoplastic and the electric field induced viscosity ($\eta_{E \neq 0}$) increases sharply. A higher particle concentration results in a denser particle structure organized in the externally applied electric field with a higher resistance against flow. The increase in the electric field induced viscosity of suspensions with increased dispersed particle concentration is due to the enhanced polarization forces between particles. The relationship between polarization forces and the electric field strength is³⁷

$$F = (6\epsilon_2 r^6 E^2) / \rho^4 \quad (3)$$

where, F is the polarization forces between the particles, ϵ is the dielectric constant, r is the radius of the suspended particles, E is the electric field strength and ρ is the distance between the suspended particles. As reflected in Eq. (3), the distance between particles decreases with increasing suspension concentration, which results in increased polarization force and undergoes to enhanced suspension's viscosity. In this study, the maximum increase in the electric field induced viscosity of suspensions was observed to change in the order: KAO ($\eta_{E \neq 0} = 215$

Pas) < PIN ($\eta_{E \neq 0} = 275 \text{ Pas}$) < PIN/KAO ($\eta_{E \neq 0} = 319 \text{ Pas}$).

Felici and Zhou reported that, suspended particles should have a definite concentration in a suspension to form fibers as a result of electric field induced polarization.^{38,39} Similar behaviors were also reported by Wu and Shen,⁴⁰ Kordonsky et al.,⁴¹ and Gow and Zukoski⁴² in ER studies of chitin/SO, chitosan/SO, carboxymethyl cellulose/transformer oil and polyaniline/SO systems, respectively.

Changes in shear stress with electric field strength

Figure 7 represents the changes in log (shear stress) (τ) with electric field strength. It was observed that, shear stress increases sharply with rising electric field strength after the threshold energy of $E_t = 1.0 \text{ kV/mm}$ was supplied. This indicates that ER suspensions form a stronger fibrillar structure under increasing electric field strength, as a result of enhanced electric field induced polarization forces.

In the present study, the maximum increase in the excess shear stress ($\Delta\tau = \tau_{E \neq 0} - \tau_{E=0}$) of suspensions was observed to change in the order: KAO ($\Delta\tau = 38.0 \text{ Pa}$) < PIN ($\Delta\tau = 43.2 \text{ Pa}$) < PIN/KAO composite ($\Delta\tau = 52.5 \text{ Pa}$). As expected the highest increase in the excess shear stress was obtained for PIN/KAO composite.

Similar behaviors were observed for polyisoprene-co-poly(*tert*-butylmethacrylate-Li)/SO system in our previous study³² and has also been reported for various other ER fluid systems such as glycerol activated titania/SO,⁴³ water doped microcrystalline nano-sized SiO_2 particle/SO,⁴⁴ poly(naphthalene quinone) radical/SO⁴⁵ and oxidized polyacrylonitrile.⁴⁶

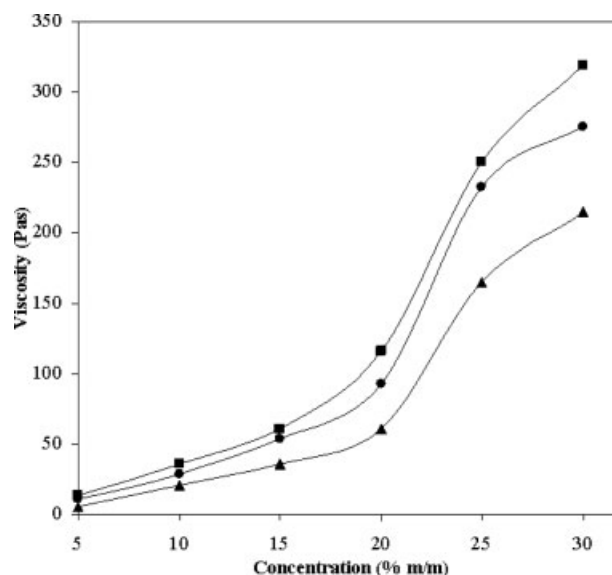


Figure 6 Effect of concentration on electric field viscosity. $\dot{\gamma} = 1.0 \text{ s}^{-1}$, $E = 2.0 \text{ kV/mm}$, $T = 25^\circ\text{C}$, (■) PIN/KAO, (●) PIN, (▲) KAO.

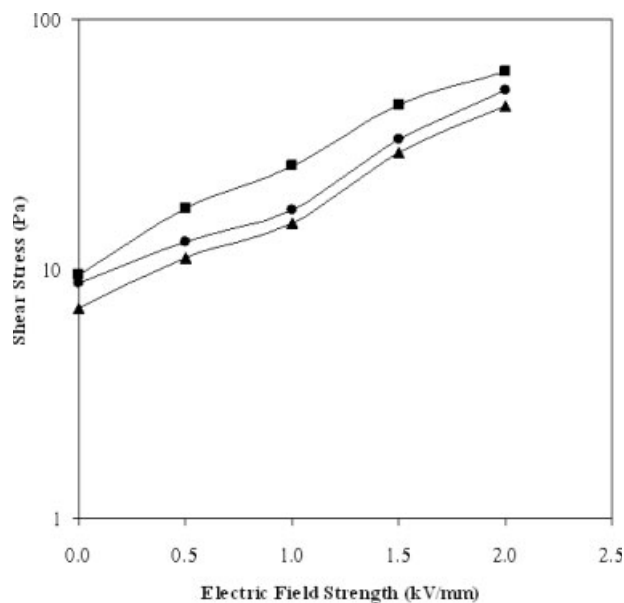


Figure 7 The change of log(shear stress) with electric field strength. $T = 25^{\circ}\text{C}$, $c = 15\%$, $\dot{\gamma} = 1.0 \text{ s}^{-1}$, (■) PIN/KAO, (●) PIN, (▲) KAO.

Changes in shear stress with concentration

The effect of suspension concentration on log (shear stress) was studied at $\dot{\gamma} = 1.0 \text{ s}^{-1}$, $T = 25^{\circ}\text{C}$ and $E = 2.00 \text{ kV/mm}$ constant conditions (Fig. 8). It was observed that, the shear stresses of the three ER suspensions examined are largely dependent on the suspended particle concentration.

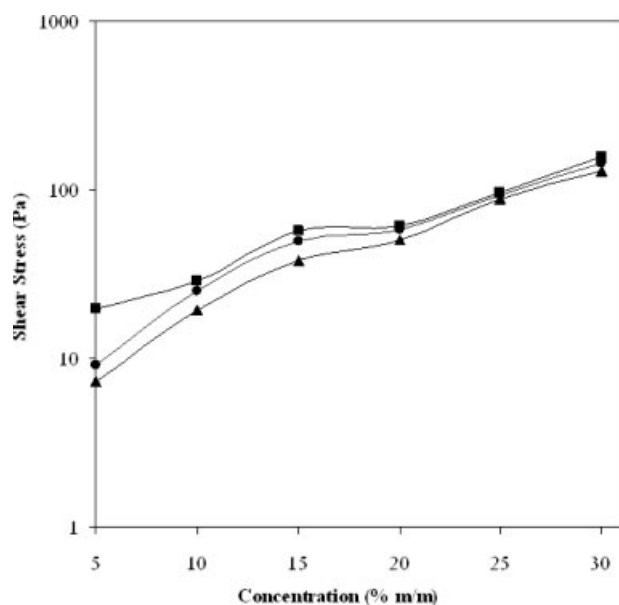


Figure 8 The change of log(shear stress) with concentration. $\dot{\gamma} = 1.0 \text{ s}^{-1}$, $T = 25^{\circ}\text{C}$, $E = 2.0 \text{ kV/mm}$, (■) PIN/KAO, (●) PIN, (▲) KAO.

In the present study, the maximum increase in the excess shear stress ($\Delta\tau$) of suspensions was observed to change in the order: KAO ($\Delta\tau = 123 \text{ Pa}$) < PIN ($\Delta\tau = 134 \text{ Pa}$) < PIN/KAO composite ($\Delta\tau = 137 \text{ Pa}$). As expected the highest increase in the shear stress was obtained for PIN/KAO/SO system.

Generally, the increase in shear stress was due to the increased polarization forces as the particle concentration was increased, which results in enhanced ER activity. These secondary forces may be stronger in the PIN/KAO composite/SO system than in the KAO/SO and PIN/SO systems.

Hiamtup derived a linear relationship between shear stress and particle concentration, on the basis of a fibrillation model.⁴⁷ Wu and Shen reported a similar trend³⁹ for chitin/SO and a chitosan/SO system, and Yin and Zhao⁴⁸ for a glycerol activated titania/SO system. Yavuz et al.¹² reported that shear stress parabolically increases with particle concentration for polystyrene-block-poly(methylmethacrylate)/SO suspension.

Effects of electric field strength on viscosity

Figure 9 illustrates the characteristic flow behavior of KAO/SO, PIN/SO and PIN/KAO/SO suspension system ($c = 15\%$) under applied external electric field. In the presence of increasing electric field strength ($E = 0.5\text{--}2.0 \text{ kV/mm}$), the flow curves become non-Newtonian and their pseudo plastic characteristic appears. Maximum electric field viscosities ($\eta_{E \neq 0}$) were observed to change in the order: KAO (52 Pas) < PIN (57 Pas) < PIN/KAO

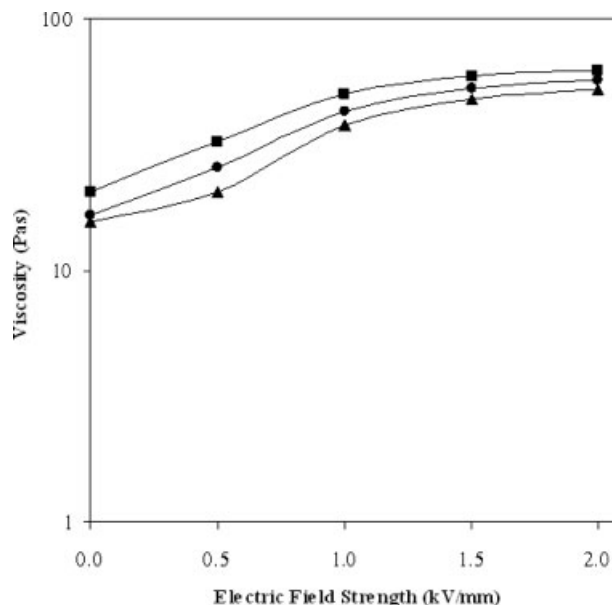


Figure 9 Effects of electric field strength on log(viscosity). $T = 25^{\circ}\text{C}$, $\dot{\gamma} = 1.0 \text{ s}^{-1}$, $c = 15\%$, (■) PIN/KAO, (●) PIN, (▲) KAO.

(62 Pas). As expected the highest $\eta_{E \neq 0}$ was obtained for the PIN/KAO/SO system.

Similar results were reported by Yavuz and Unal,³² Yang and Huang⁴⁹ for ER suspensions of polyisoprene-*co*-poly(*tert*-butylmethacrylate-Li)/SO, poly(*n*-hexyl isocyanate)/*o*-xylene and polyaniline/SO systems, respectively.

Change in viscosity with shear rate

Change of log(viscosity) and log(shear stress) of KAO/SO, PIN/SO and PIN/KAO/SO suspensions with shear rate at constant conditions ($c = 15\%$, $E = 2.0$ kV/mm, $T = 25^\circ\text{C}$) is shown in Figure 10. As is evident, electric field viscosities of the suspensions decrease sharply with increasing shear rate up to $\dot{\gamma} = 1.0$ s⁻¹ and giving a typical curve of shear thinning non-Newtonian visco-elastic behavior. After $\dot{\gamma} > 1.0$ s⁻¹, gradual decreases in the viscosities of the suspensions were observed with increasing shear rate. Under an applied shearing force, particles are affected by viscous forces, due to the hydrodynamic interactions of particles in the suspensions. Similar results are reported by Espin and Rejon for hematite/SO system.⁵⁰

Effect of temperature and promoter on shear stress

The temperature dependence of the shear stresses for the suspensions studied in this work is shown in Figure 11. The results were obtained at temperatures of 25, 50, 75, 100, and 125°C. It was observed that the shear stresses slightly decrease with rising temperature.

The effect of temperature is one of the most important parameter to evaluate ER phenomena.³⁹ Gen-

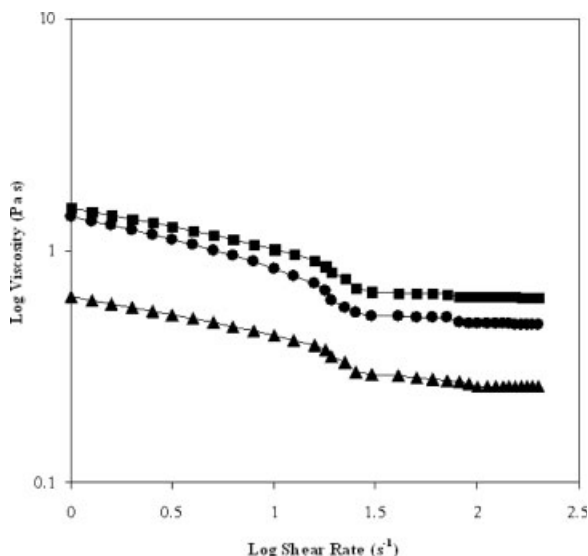


Figure 10 The change of log (viscosity) with log (shear rate). $T = 25^\circ\text{C}$, $E = 2.0$ kV/mm, $c = 15\%$, (■) PIN/KAO, (●) PIN, (▲) KAO.

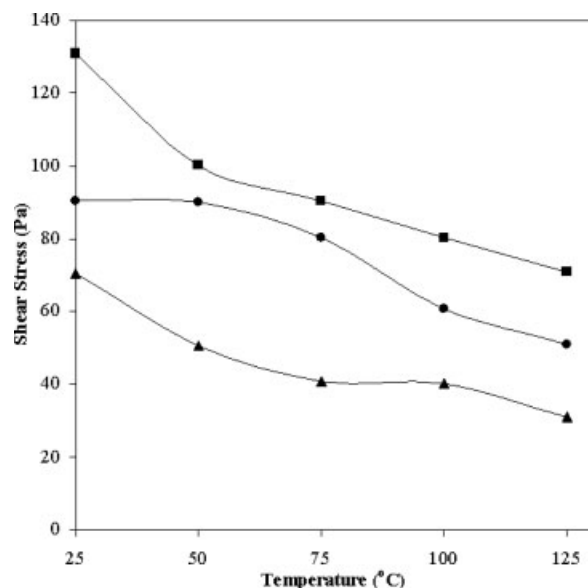


Figure 11 Effect of temperature on shear stress. $\dot{\gamma} = 1.0$ s⁻¹, $E = 2.0$ kV/mm, $c = 15\%$, (■) PIN/KAO, (●) PIN, (▲) KAO.

erally, the temperature has two effects on the ER fluids: one is the effect on the polarization intensity of particle and other one is the Brownian motion. The increase of the temperature results, both in decreased activation energy of polarization of suspended particles and, also on the polarizability of the particles, which results with a decrease in the ER strength of the suspensions. On the other hand, Brownian motion does not contribute to the chain formation for KAO, PIN, and PIN/KAO composite particles, dispersed in SO.

The shear stress losses between 25 and 125°C are also calculated and given in Table IV. Minimum shear stress loss ($\Delta\tau = 30.94$ Pa) was observed for KAO/SO suspension, which may be attributed to the stronger electric field induced fibrillar structure formation in the suspension. These observations are consistent with the results reported by Choi for chitosan/SO,⁵¹ Unal and Yilmaz¹¹ for poly(methylmethacrylate)-block-polystyrene/SO and by Yilmaz and coworkers¹⁸ for poly(2-hydroxy ethylmethacrylate)/SO suspensions.

The effect of added polar promoters on the shear stresses of the suspensions were also investigated by

TABLE IV
Effect of Temperature on Shear Stress Loss

Sample	Shear Stress Loss (Pa)
KAO	39.50
PIN	39.40
PIN/KAO composite	59.90

$\dot{\gamma} = 1.0$ s⁻¹, $E = 2.0$ kV/mm, and $c = 15\%$.

adding various promoters into the suspensions (i.e., water, alcohol, glycerol), and no promoting effect was observed. That is why the system studied in this work was classified as a dry ER system, which is very important result from industrial stand point.

CONCLUSIONS

Maximum colloidal stability was obtained for PIN/KAO composite/SO system as 72 days ($c = 5\%$).

Flow times of suspensions observed to increase with increasing electric field strength and suspension concentration.

ER activity of all the suspensions was observed to increase with increasing electric field strength, concentration and decreasing shear rate.

Shear stress was found to sharply increase with increasing electric field strength and suspension concentration.

The electric field viscosity of all the suspensions was decreased sharply with increasing shear rate and showing a typical shear-thinning non-Newtonian visco-elastic behavior.

High temperature was observed to slightly decrease the shear stress of the suspensions.

ER activities of the suspensions were observed not be affected from various promoters and the systems investigated are classified as dry ER fluids.

References

- Tao, R.; Sun, M. J. *Phys Rev Lett* 1991, 67, 398.
- Sakurai, R.; See, H.; Saito, T.; Asai, S.; Sumita, M. *Rheol Acta* 1999, 38, 478.
- Hao, T.; Kawai, A.; Ikazaki, F. *Int J Mod Phys B* 1999, 13, 1758.
- Cho, M. S.; Choi, H. J.; Chin, I. J.; Ahn, W. S. *Microporous Mesoporous Mat* 1999, 32, 233.
- Choi, H. J.; Kim, W. J.; Yoon, S. H.; Fujiura, R.; Komatsu, M.; Jhon, M. S. *J Mater Sci Lett* 1999, 18, 1445.
- Block, H.; Kelly, P. J.; Qin, A.; Watson, T. *Langmuir* 1990, 6, 6.
- Hiamtup, P.; Sirivat, A.; Jamieson, A. M. *J Colloid Interface Sci* 2006, 295, 270.
- Kim, W. J.; Kim, S. G.; Choi, H. J.; Jhon, M. S. *Macromol Rapid Commun* 1999, 20, 450.
- Choi, H. J.; Kim, W. J.; To, K. *Synth Met* 1999, 101, 697.
- Trlica, J.; Saha, P.; Quadrat, O.; Stejskal, J. *Physica A* 2000, 283, 337.
- Unal, H. I.; Yilmaz, H. *J Appl Polym Sci* 2002, 86, 1106.
- Yavuz, M.; Unal, H. I.; Yildirim, Y. *Turk J Chem* 2001, 25, 19.
- Lim, Y. T.; Park, H. J.; Park, O. O. *J Colloid Interface Sci* 2002, 245, 198.
- Yilmaz, H.; Unal, H. I.; Yavuz, M.; Arik, H. *Gazi Univ J Sci* 2003, 16, 473.
- Yilmaz, H.; Unal, H. I. *J Appl Polym Sci* 2006, 99, 3540.
- Yilmaz, H.; Unal, H. I. *J Appl Polym Sci* 2006, 101, 1065.
- Yilmaz, H.; Degirmenci, M.; Unal, H. I. *J Colloid Interface Sci* 2006, 293, 489.
- Unal, H. I.; Agirbas, O.; Yilmaz, H. *Colloids Surf A Physicochem Eng Asp* 2006, 274, 77.
- Zhao, X. P.; Duan, X. *Mater Lett* 2002, 54, 348.
- Hao, T.; Yu, H.; Xu, Y. *J Colloid Interface Sci* 1996, 184, 542.
- Woo, D. J.; Kim, J.; Suh, M.; Zhou, H.; Nguyen, S. T. *Polymer* 2006, 47, 3287.
- Kesy, Z.; Kesy, A.; Plochanski, J.; Jackson, M.; Parkin, R. *Mechatronics* 2006, 16, 33.
- Lim, S.; Park, S. M.; Kim, K. *J Sound Vib* 2005, 284, 685.
- Shchipunov, Y. A.; Dürrschmidt, T.; Hoffmann, H. *J Colloid Interface Sci* 1999, 212, 390.
- Kawasumi, M.; Hasegawa, N.; Koto, M.; Usuki, A.; Okada, A. *Macromolecules* 1997, 30, 6333.
- Tunney, J. J.; Detellier, C. *Chem Mater* 1996, 8, 927.
- German, R. M. *Powder Metallurgy Science, Metal Powder Industries, Federation, Princeton*, 1994; p 28.
- Talbi, H.; Maarouf, E. B.; Humbert, B.; Alnot, M.; Ehrhardt, J. J.; Ghanbaja, J.; Billaud, D. *J Phys Chem Solids* 1996, 57, 1145.
- Johnston, C. T.; Sposito, G.; Bocian, D. F.; Birge, R. R. *J Phys Chem* 1984, 88, 5964.
- Palaniappan, S.; Narayana, B. H. *J Polym Sci Part A: Polym Chem* 1994, 32, 2431.
- Hao, T. *Adv Colloid Interface Sci* 2002, 97, 1.
- Yavuz, M.; Unal, H. I. *J Appl Polym Sci* 2004, 91, 1822.
- Yilmaz, H.; Unal, H. I.; Yavuz, M. *Colloid J* 2005, 67, 236.
- Uemura, T.; Minagawa, K.; Takimoto, J. *J Chem Soc Faraday* 1995, 91, 1051.
- Rejon, L.; Ramirez, A.; Paz, F.; Goycoolea, F. M.; Valdez, M. A. *Carbohydr Polym* 2002, 48, 413.
- Unal, H. I.; Yavuz, M.; Yilmaz, H.; Gazi Univ J Sci 2001, 14, 999.
- Bezruk, V. I.; Lazarev, A. N.; Malov, V. A.; Usyarov, O. G. *Colloid J* 1972, 34, 142.
- Felici, N. J. *J Elektrostat* 1997, 40, 567.
- Li, J. R.; Zhou, L.; Liu, H. *Solid State Commun* 1998, 107, 561.
- Wu, S.; Shen, J. *J Appl Polym Sci* 1996, 60, 2159.
- Kordonsky, V. I.; Korobko, E. V.; Lazareva T. G. *J Rheol* 1991, 35, 1427.
- Gow, C.; Zukoski, C. F. *J Colloid Interface Sci* 1990, 136, 175.
- Yin, B. J.; Zhao, X. P. *J Colloid Interface Sci* 2003, 257, 228.
- Liu, Y.; Liao, F.; Li, J.; Zhang, S.; Chen, S. *Scripta Mater* 2006, 54, 125.
- Cho, M. S.; Choi, H. J. *Korea-Australia Rheol J* 2000, 12, 151.
- Hao, T.; Xu, Y. *J Colloid Interface Sci* 1997, 185, 327.
- Hiamtup, P.; Sirivat, A.; Jamieson, A. M. *J Colloid Interface Sci* 2006, 295, 270.
- Yin, B. J.; Zhao, X. P. *J Colloid Interface Sci* 2003, 257, 228.
- Yang, I. K.; Huang, I. T. *J Polym Sci Part B: Polym Phys* 1997, 35, 1217.
- Espin, M. J.; Delgado, A. V.; Rejon, L. *J Non-Newton Fluid Mech* 2005, 125, 1.
- Choi, U. *Colloids Surf A: Physicochem Eng Asp* 1999, 157, 193.